

# Vacuum-sealed miniature modulated x-ray source and the influence factors of x-ray intensity

Baoquan Li (李保权)<sup>1,2</sup> and Huan Mou (牟欢)<sup>1,2,\*</sup>

<sup>1</sup>National Space Science Center, Chinese Academy of Science, Beijing 100190, China

<sup>2</sup>University of Chinese Academy of Science, Beijing 100190, China

\*Corresponding author: mouhuan@nssc.ac.cn

Received January 7, 2016; accepted May 5, 2016; posted online May 31, 2016

The vacuum-sealed miniature modulated x-ray source (VMMXS) with a hot cathode is fabricated via the single-step brazing process in a vacuum furnace. An experiment following the VMMXS is implemented to present its performances, including the influence of grid electrode potential on x-ray intensities. The modulation type of the grid electrode as a switch is proposed, and its feasibility is successfully demonstrated. It is noteworthy to discover a phenomenon for the first time, to the best of our knowledge, that the high repetition frequency grid pulse of the VMMXS has a significant effect on the x-ray intensity. The probable cause for this new finding is analyzed.

OCIS codes: 340.7480, 230.6080, 260.6048, 300.6560.

doi: 10.3788/COL201614.073401.

The x ray has a strong penetrating power, almost without attenuation for transmission in outer space, so it is a convincing use of x-ray communication in inter-satellite or deep space. As a new concept for space communication, there will be more important scientific significance and application prospects called “Next-Generation Communications”. The vacuum-sealed miniature modulated x-ray source (VMMXS) assembly is one of the many parts of the x-ray communication system, whose traffic rate is determined by the modulation rate of the VMMXS assembly. Hence, it is meaningful to develop the VMMXS system.

Recently, the carbon nanotube (CNT) has been extensively used for electron sources of traditional x-ray tubes in the burgeoning field of nanomaterials<sup>[1]</sup>. However, it isn't suitable for high frequency modulated x-ray sources based on a fully vacuum-sealed tube. First, it is very exponentially susceptible to a poor vacuum ambience because it must continue to emit electrons stably at a vacuum level below  $1 \times 10^{-5}$  Pa<sup>[2-4]</sup>. Therefore, there are few reports on fully vacuum-sealed x-ray tubes (FVSXTs) without active pumping systems<sup>[5]</sup>. Most recently, an FVSXT based on CNT field emitters has been developed<sup>[6,7]</sup>. Second, they do not generally emit electrons unless the gate voltage exceeds a certain value, which is usually at the level of kilovolts (kV)<sup>[6-8]</sup>. An x-ray pulse with a repetition rate greater than 20 kHz has been achieved by modulating the gate voltage with a high voltage pulse source (HVPS)<sup>[9,10]</sup>. Additionally, the power dissipation of an HVPS is too high to cool it with chillers. The 2 kV pulse generator with a 35 kHz repetition rate corresponds to a switch heating rate of 80 W. These deficiencies make vacuum brazing of CNT FVSXT more difficult, and limit the modulation frequency of modulated x-ray source.

In contrast, the greatest advantage of the so-called “hot cathode”, usually a tungsten (W) filament, is that it allows free electrons to escape from the surface in non-high

vacuum (non-HV) circumstances, even at a pressure of  $1 \times 10^{-3}$  Pa. It, the robustness for the hot cathode in non-HV, indeed makes the vacuum brazing of the x-ray tube without an active pump easier. Furthermore, there is no need to use HVPS. The grid-controlled pulse x-ray source based on the hot cathode has been designed and modulated by a lower power dissipation pulse generator, which merely satisfies the voltage amplitude of above 10 V<sup>[11-13]</sup>.

Here, we report on a detailed study on the VMMXS assembly, which is programmed by a pulsed signal loaded onto the grid electrode and generating x ray with a micrometer-sized focal spot, with a hot cathode. An experiment has been implemented to verify its performance. The verification of feasibility founded on grid electrode modulation is also involved. Meanwhile, we discover for the first time, to the best of our knowledge, that the high frequency grid pulse of the VMMXS has a significant effect on the x-ray intensity, according to the searchable literature.

Figure 1(a) shows a schematic of the designed VMMXS and its simulation results for electron beam trajectories using commercial software. Basically, the VMMXS is made up of a hot cathode (usually a tungsten filament), a grid electrode, three focusing electrodes, a connecting anode, and a transmission-type x-ray target plated on a beryllium window embedded in the connecting anode. The grid electrode resembles a switch used for permitting electrons from the hot cathode to transit or not. Electrons are restrained from passing when the negative grid voltage is loaded. As shown in Fig. 1(b), not even one of the innumerable electrons is allowed to pass so long as the grid voltage is inferior to  $-1$  V. While set up with a positive voltage, the grid electrode lets electrons get through. In addition, the electron number getting through the grid electrode is determined by the grid voltage and the power consumption of the tungsten filaments. Provided that

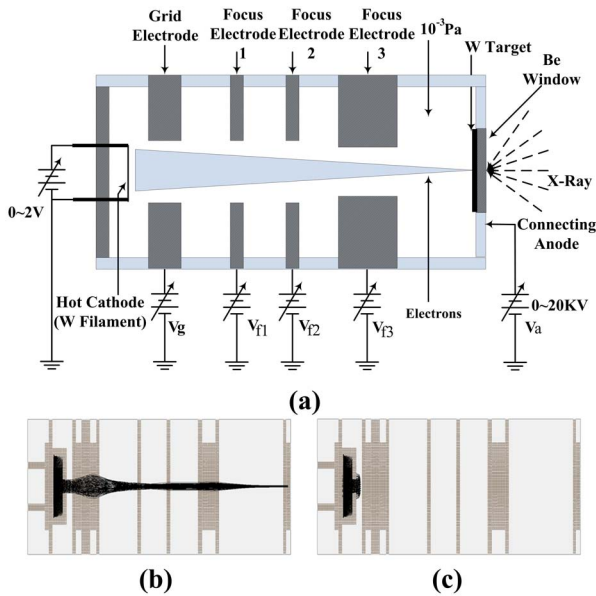


Fig. 1. (a) Schematic of the VMMXS system. (b) Simulated electron beam trajectories for the VMMXS with the positive grid value. (c) Simulated electron beam trajectories with the negative grid value.

there are electrons getting through the grid electrode, the electron beam must be induced by three different focus electric fields. As a result, the diameter of the electron beam diminishes gradually while it gets through the three focus electrodes. Finally, it focuses onto the tungsten target, and then generates x rays with a micrometer-sized focal spot. The physical dimension and the relative positions of all parts of the VMMXS and these voltages, separately loaded on different electrodes, are repeatedly simulated and optimized to aim at the lower grid voltage as a switch and the smaller diameter of the focal spot.

Additionally, a transmission-type target for the VMMXS is adopted to try to attain a small x-ray focal spot<sup>[9]</sup>. Besides, the precise position of the x-ray focal spot is more easily achieved in a VMMXS with a transmission-type target than that with a reflection-type target. The thickness of a transmission-type target should be considerable, considering that it is the key parameter influencing the conversion efficiency of the x ray. If the target thickness is too thin, only part of the incident electrons are converted into x rays, while most of them get through the target material without transformation. But, x rays translated from incident electrons obviously attenuate when the target thickness exceeds a certain constant, which is called the optimum target thickness (OTT). When the thickness is thicker than the OTT, the x rays will be absorbed by the target material although all incident electrons convert into x rays. So, it's necessary to find the OTT for the sake of increasing the conversion efficiency of x rays. Moreover, the OTT is determined by the material of the targets and the incident electron energy (depending on the anode voltage). Therefore, given the incident electrons of 15 KeV of energy, the OTT of tungsten

is simulated via particle transport software using the Monte Carlo method, and finally determined to be  $0.3 \mu\text{m}$ .

Figure 2(a) shows an optical photograph of the full VMMXS assembly (20 mm in diameter and 75 mm in length), in which the grid electrode, three focus electrodes, and the connecting anode are made of Kovar, chosen because of its thermal expansion coefficient proximate with the ceramic of  $\text{Al}_2\text{O}_3$ . Five  $\text{Al}_2\text{O}_3$  ceramic tubes are adopted to insulate all electrodes. All components of the VMMXS are baked at  $550^\circ\text{C}$  for 10 h, and subsequently, they are brazed through a single-step brazing process at  $680^\circ\text{C}$  in a vacuum furnace. Afterwards, the VMMXS system works steadily without a discernible decline in the generating x ray. The x-ray energy spectra radiated from the tungsten target is monitored with a silicon drift detector (Amptek X-123SDD). The characteristic spectrum, which happens when electrons from higher energy levels fill up the vacancy that exists because of orbital electrons knocked out of the inner electron shell of a metal atom, superimposes on the continuous spectrum due to bremsstrahlung. The characteristic spectra of tungsten elements are displayed in Fig. 2(b), including  $L\tau$ ,  $L\alpha_1$ ,  $L\alpha_2$ ,  $L\beta_1$ ,  $L\beta_2$ , and  $L\gamma_1$ , in which  $L\alpha_1$  and  $L\alpha_2$  aren't distinguished because of the subtle energy difference between them. The x-ray intensity is controlled by the power consumption of the tungsten filaments and the grid voltage. So, the only limitation for the x-ray intensity is the power consumption of a tungsten filament, given a grid voltage. The emission property of the tungsten filament

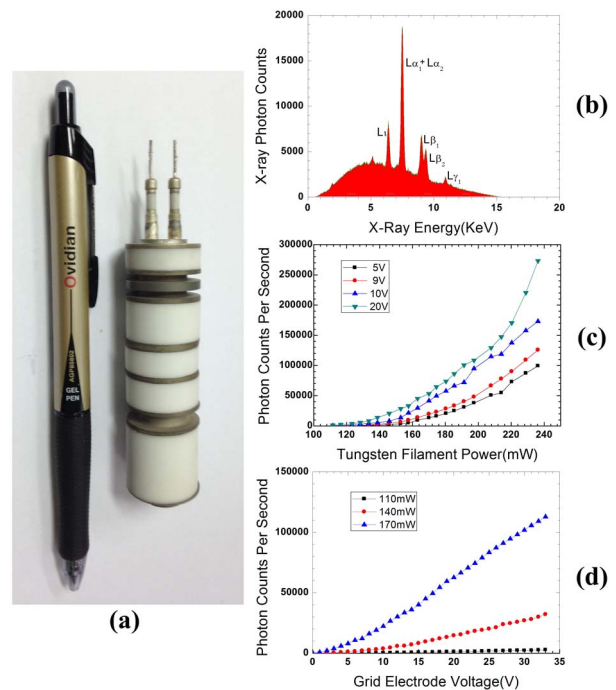


Fig. 2. (a) Optical photograph of the full VMMXS assembly. (b) X-ray energy spectra of the tungsten target. (c) Photon counts versus cathode power consumption characteristics of the VMMXS. (d) Photon counts versus grid voltage characteristics of the VMMXS.

is exhibited in Fig. 2(c), which shows that the number of x-ray photons increases exponentially along with the increasing heat dissipation of the tungsten filament. Four curvilinear relationships, coinciding with the curve profile of the hot electron emission current versus the temperature of the tungsten filament, correspond to four grid voltages (5, 9, 10, and 20 V, respectively). In addition, the photon number is merely concerned with the grid voltage for preset hot cathode power consumption. It is revealed in Fig. 2(d) that the photon number augments linearly following the raising of the grid voltage. The slope is limited by the given heat dissipation of the cathode. So it is further promising to adopt amplitude modulation of the grid voltage rather than pulse modulation as a switch, considering the approximate linear relationship between the photon number and the grid voltage.

It is authenticated in Fig. 3 that it is feasible to modulate the VMMXS system via installing the modulating signal on the grid electrode. (a) The yellow waveform is the input modulating signal (IMS), while (b) the purple one is the output of the multi-channel analyzer (MCA), a kind of x-ray detector, which produces a short voltage spike corresponding to each detected photon without filtering. A burst of x ray generates and is detected for each logic, namely, the IMS is positive. There is no burst of voltage spikes exiting except some white noise, as the IMS is negative. Moreover, the irregularity of the individual voltage spikes is limited by the different energies of the detected photons because the amplitude of the voltage spikes coincides with the energy of the photons. Therefore, the feasibility of grid modulation to the VMMXS has been tested by the experiment. The 50 kHz modulation frequency has been achieved, which is restrained by the amplitude of the IMS and the power consumption of the hot cathode for a given anode voltage. Furthermore, it is verified in an earlier study that the individual x-ray pulse is expected to be consistent with the electron, produced from an exceptional femtosecond laser source jittered with less than a 200 ps pulse width, with hardly a timing delay<sup>[14–18]</sup>. So it is conceivable for gigahertz (GHz) level modulation frequency for the VMMXS in the future, provided there are enough incident electrons.

During the confirmatory experiment of the grid modulation's feasibility, a particular phenomenon has been

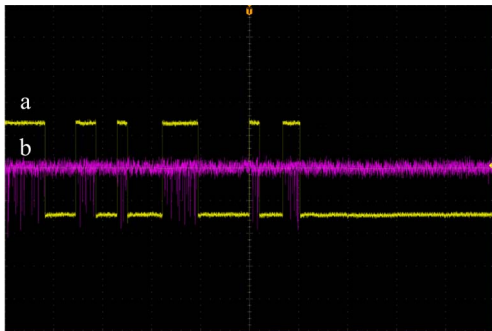


Fig. 3. Pulsed width and modulation rate of the x ray are controlled by modulating the grid electrode.

initially discovered; the repetition frequency of grid pulses has an important influence on the detected x-ray intensity in accordance with the investigative papers. The square-wave pulse is preset with the amplitude of 9 V and the on-off ratio of 50%. Consequently, as revealed in Fig. 4(a), the detected photon number is changing along with the change of grid pulse frequency from 1 to 20 MHz, of which the frequency range is constrained by the adopted signal generator. There are two peaks of x-ray photon counts in the chart: one of these peak numbers is 170000 per second on the condition of an 8 MHz grid pulse repetition frequency, and the other reaches up to 260000 at 15 MHz. However, it is obvious in Fig. 2(d) that the detected photon number is less than 20000 when provided with 9 V of direct voltage on the grid electrode. It is interesting that the only difference in loading the square wave of a 15 MHz grid frequency rather than direct voltage at the same amplitude makes the generated x-ray intensity rise more than one order of magnitude. Most of the pulses with a different repetition frequency urge the detected photon numbers to exceed 20000.

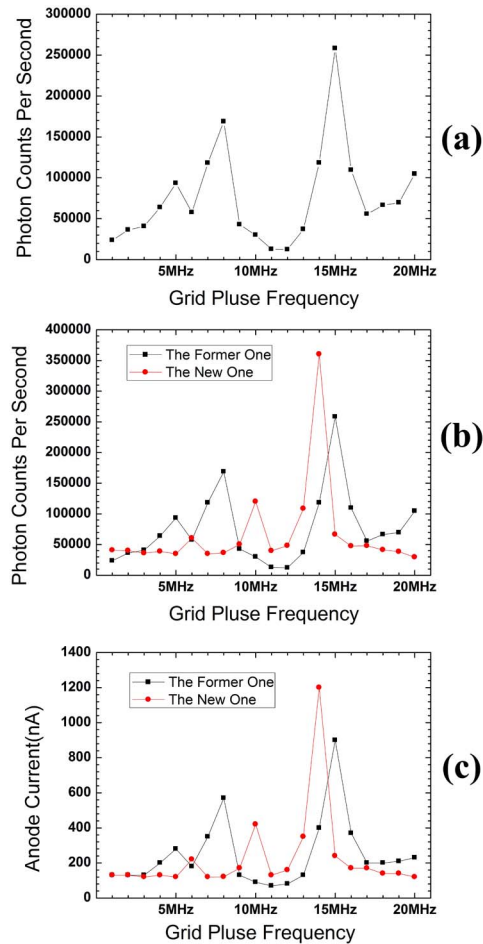


Fig. 4. (a) Photon counts versus the grid pulse frequency characteristics of the VMMXS. (b) Photon counts versus grid pulse frequency contrastive characteristics between the former one and the new one. (c) Anode current versus grid pulse frequency contrastive characteristics between the former one and the new one.

To corroborate that the phenomenon not an accident, a new VMMXS is manufactured. All factors of these two VMMXS are the same, excluding the tungsten filament dimensions. Subsequently, this particular phenomenon has appeared again in the new VMMXS, and it is illustrated in Fig. 4(b), in which two curves of the original and the new one are revealed contrastively. There are also two peaks in the new one, and their grid pulse frequencies move to 10 and 14 MHz from 8 and 15 MHz, respectively. The produced x-ray number with the 14 MHz grid pulse frequency is almost one order of magnitude higher than that with direct voltage. Meanwhile, the anode current of these VMMXS are measured, and the result is showed in Fig. 4(c). It is also obvious that two peaks of anode current exist, and their curves are identical with those of produced x-ray counts. So it is confirmed again that certain repetition frequencies of grid pluses make the VMMXS produce many more x rays.

After excluding some possibilities via repeating experiments, it is finally concluded that the most likely cause of this particular phenomenon is that high repetition frequency pulses, especially certain frequencies, make heating a tungsten filament generate more incident electrons, which are accelerated and will then produce more x rays with the same transfer efficiency. However, the reason for the appearance of two peaks of incident electron numbers at the range of 20 MHz for each VMMXS is currently incomprehensible. It is probable that other peaks exist at frequencies exceeding 20 MHz. Furthermore, these frequencies corresponding with peaks vary along with dimensions of the tungsten filaments. Although reasons for the particular phenomenon are not clear at present, the discovery is far-reaching anyway. As a result, the electron emission efficiency, one of the biggest disadvantages of a hot cathode, can be sharply improved more than ten times by loading pulses of certain frequencies, which might be widely used in generating further x rays. It might be also applied in the VMMXS to increase the maximum modulation frequency. Even though resonance vibration, which should be generally avoided, gives rise to creating more electron emissions, it is meaningful for this finding as well. It can provide a factor to be considered by scientific research personnel, and remind them of whether or not they should evade resonance frequency according to the purpose of their research.

In conclusion, the VMMXS is designed and optimized by simulation, and finally manufactured via the single-step brazing process. The feasibility of grid pulse modulation is demonstrated, and a 50 kHz modulation frequency is accomplished with the limitation of power

consumption and electron emission efficiency of a hot cathode. Additionally, it is significant to initially discover that certain repetition frequencies of grid pulses make the VMMXS produce more x rays. It might be used in improving the modulation frequency of the VMMXS or the x-ray intensity of traditional x-ray sources in the future. The VMMXS could be extensively applied to pulsar simulation, inter-satellite x-ray communication, and ionization blackout area communication.

We thank Yong-tao Yuan for the coating tungsten of the transmission-type anode target.

## References

1. Z. Liu, G. Yang, Y. Z. Lee, D. Bordelon, J. Lu, and O. Zhou, *Appl. Phys. Lett.* **89**, 103111 (2006).
2. A. Haga, S. Senda, Y. Sakai, Y. Mizuta, S. Kita, and F. Okuyama, *Appl. Phys. Lett.* **84**, 2208 (2004).
3. S. Senda, Y. Sakai, Y. Mizuta, S. Kita, and F. Okuyama, *Appl. Phys. Lett.* **85**, 5679 (2004).
4. H. Sugie, M. Tanemura, V. Filip, K. Iwata, K. Takahashi, and F. Okuyama, *Appl. Phys. Lett.* **78**, 2578 (2001).
5. Y.-H. Song, J.-W. Kim, J.-W. Jeong, J.-T. Kang, S. Choi, K. E. Choi, and S.-J. Ahn, in *IEEE 25th International Vacuum Nanoelectronics Conference*, Jeju, Korea (2012), pp. 102.
6. J.-W. Jeong, J.-W. Kim, J.-T. Kang, S. Choi, S. Ahn, and Y.-H. Song, *Nanotechnol.* **24**, 085201 (2013).
7. S. H. Heo, A. Ihsan, and S. O. Cho, *Appl. Phys. Lett.* **90**, 183109 (2007).
8. J.-T. Kang, H.-T. Lee, J.-W. Jeong, J.-W. Kim, S. Park, M.-S. Shin, J.-H. Yeon, and H. Jeon, *IEEE Electron. Device Lett.* **36**, 1209 (2015).
9. Y. Cheng, J. Zhang, Y. Z. Lee, B. Gao, and S. Dike, *Rev. Sci. Instrum.* **75**, 3264 (2004).
10. G. Z. Yue, Q. Qiu, B. Gao, Y. Cheng, and J. Zhang, *Appl. Phys. Lett.* **81**, 355 (2002).
11. D. Ning-Qin, Z. Bao-Sheng, and S. Li-Zhi, *Acta Phys. Sin.* **62**, 060705 (2013).
12. M. Xiao-Fei, Z. Bao-Sheng, S. Li-Zhi, L. Yong-An, L. Duo, and D. Ning-Qin, *Acta Phys. Sin.* **63**, 160701 (2014).
13. S. Li-zhi, Z. Bao-sheng, and L. Yong-an, *Proc. SPIE* **9207**, 920716 (2015).
14. S. M. Foreman, C. Kealhofer, G. E. Skulason, B. B. Klopfer, and M. A. Kasevich, *Ann. Phys.* **525**, 19 (2013).
15. Y. Tian, W. Wang, C. Wang, X. Lu, C. Wang, Y. Leng, and X. Liang, *Chin. Opt. Lett.* **11**, 033501 (2013).
16. J. Wang, Z. Zhao, W. He, B. Zhu, K. Dong, Y. Wu, T. Zhang, and G. Niu, *Chin. Opt. Lett.* **13**, 031001 (2015).
17. U. Hinze, A. Egbert, B. Chichkov, and K. Eidmann, *Opt. Lett.* **29**, 2079 (2004).
18. M. Nishikino, N. Hasegawa, M. Ishino, Y. Ochi, T. Kawachi, M. Yamagiwa, and Y. Kato, *Chin. Opt. Lett.* **13**, 070002 (2015).